RSC Advances

ROYAL SOCIETY OF CHEMISTRY

www.rsc.org/advances

Catalytic Cracking of Jatropha-Derived Fast Pyrolysis Oils with VGO and their NMR Characterization

Desavath V. Naik[a], Vimal Kumar[b],[1] Basheshwar Prasad[b], Mukesh K. Poddar[a], Rajaram Bal[a], Babita Behera[a], Om.P. Khatri[a], D.K. Adhikari[a] , M.O. Garg[a]

[a]*Bio-fuels Division, CSIR-Indian Institute of Petroleum, Dehradun 248005, India*

[b]*Department of Chemical Engineering, Indian Institute of Technology Roorkee, Roorkee 247667, India*

Abstract

Lignocellulosic biomass-derived fast pyrolysis oils are potential second-generation bio-fuels towards the reduction of greenhouse gas (GHG) emissions and carbon foot prints. This study pertains to co-process the Jatropha-derived heavy or tar fraction of fast pyrolysis oil (FPO) with vacuum gas oil (VGO) and hydrodeoxygenated fast pyrolysis oil (HDO) with VGO in a standard refinery fluid catalytic cracking (FCC) unit. The crude fast pyrolysis oil from jatropha curcas is produced at 530 $^{\circ}$C temperature and atmospheric pressure using a bubbling fluidized bed pyrolyzer. The heavy fraction of FPO is hydrodeoxygenated over Pd/Al_2O_3 catalyst into HDO in an autoclave reactor at 300 $^{\circ}$C temperature and 80 bar pressure. Further, the HDO is co-processed with petroleum-derived VGO in an advanced cracking evaluation (ACE-R) unit to convert them into refinery FCC product slate hydrocarbons at a blending ratio of 5:95. The FPO and HDO are characterized using ^{31}P NMR; whereas FCC distillates on co-processing of VGO with fast pyrolysis oil and HDO are characterized using ^{1}H and ^{13}C NMR spectroscopy techniques.

[1] *Corresponding author E-mail:* vksinfch@iitr.ac.in

The ^{31}P NMR analysis of crude FPO and HDO indicated that hydroxyl, carboxylic and methoxy groups are reduced during hydrodeoxygenation of FPO. The experimental results at iso-conversion level on co-processing of HDO with VGO indicated higher yield of liquefied petroleum gases (LPG), while lower yields of gasoline and LCO have been observed as compared to FPO co-processing with VGO and co-processing of pure VGO. Furthermore, the results of co-processing of FPO with VGO indicated that the yields of gasoline and LCO are increased from 29 to 35 wt.% and 14.8 to 20.4 wt.%, respectively; whereas the yields of dry gas and LPG are decreased from 2.1 to 1.4 wt.% and 38.8 to 23.7 wt.%, respectively, for an increase in the blending ratio from 5 to 20 %. Therefore, it can be concluded that the co-processing of HDO with VGO in FCC unit would be feasible in order to achieve higher yield of LPG.

Keywords: *Pyrolysis oil, HDO, Gasoline, fast pyrolysis, fluid catalytic cracking, NMR*

1.0 Introduction

The worldwide consumption of liquid fuels is bound to increase from 87 to 97 million barrels per day from 2010 to 2020, respectively and it is projected to 115 million barrels per day in 2040 [1]. The proved world oil reserves were estimated to be ~1638 billion barrels as of January 1, 2013 [2]. The world oil reserves could deplete soon in coming decade with the present rate of consumption. Hence, the research is focusing on second generation bio-fuels (besides other resources) for the production of liquid fuels from lignocellulosic biomass. Therefore, the conventional (thermal) fast pyrolysis route is an effective approach to convert biomass into higher yields (50 to 75 wt.%) of liquid fraction (crude fast pyrolysis oil) at atmospheric pressure and moderate temperature of ~500 $^{\circ}$C. The crude fast pyrolysis oil as such cannot be used as a liquid fuel due to its lower heating value (15-20 MJ/kg) and the presence of oxygenated

compounds that self-react during handling at ambient temperatures to form larger molecules [3-4]. The crude fast pyrolysis oil is a complex mixture of water, carboxylic acids, hydroxy-aldehydes, hydroxy-ketones, phenolics, guaiacols, catechols, syringols, vanilins, sugars, and levoglucosan [5]. Therefore, crude fast pyrolysis oil requires further upgrading in order to convert it into usable liquid hydrocarbons.

Thereby, a number of upgrading technologies have been proposed in the last decades, such as thermal treatment [6-7], high pressure thermal treatment [8-9], thermal hydrotreating [10], catalytic hydrotreating [11-15], catalytic emulsion [16], and catalytic cracking [17-19]. Among the aforementioned upgrading techniques, catalytic cracking seems to be a good option for effective use of trillion dollars refinery infrastructure as well as integration of fast pyrolysis process with refinery [20]. A critical review has been published by Talmadge et al. [21] on outlook of how to modify the overall chemistry of biomass-derived pyrolysis liquids in order to integrate pyrolysis process with standard petroleum refineries. Chen et al. [22] reported that the effective hydrogen index (H/C_{eff}) should be above the inflection point of 1.2 for energy production, either processing or co-processing the biomass-derived fast pyrolysis oil with petroleum-derived VGO or LCO in fluid catalytic cracking unit. Therefore it is necessary to partially deoxygenate the fast pyrolysis oil to reduce the oxygen level in order to improve the H/C_{eff} of pyrolysis oil for better processing in FCC units. Huber et al. [7] proposed that the reaction mechanism on cracking of oxygenated molecules over FCC catalyst leads to smaller hydrocarbons and coke by adding a dehydration reaction in addition to conventional hydrocarbon cracking reactions such as cracking, hydrogen consuming and producing reactions and Diels-Alder (C-C bond formation) reactions. Fogassay et al. [23] also proposed a simplified reaction mechanism for oxygen removal from biomass-derived molecules.

The conventional FCC technology is aimed to improve the gasoline yield, however while co-processing the fast pyrolysis oil with VGO it is very much essential to look into the product characterization and also the causes of coke formation. Samolada et al. [10] co-processed the hydrotreated flash pyrolysis oil (a heavy fraction) with light cycle oil (LCO) for 15:85 blending ratio in a modified MAT fixed bed reactor system (MAT, ASTM D3907-80) over FCC (ReUSY2) catalyst. An increase in coke and gasoline production by 32 and 56%, respectively, was reported while co-processing hydrotreated flash pyrolysis oil (a heavy fraction) with LCO as compared to the pure LCO processing. Fogassy et al. [23] reported a higher dry gas and coke yields, lower LPG yields, similar yields of gasoline and LCO while co-processing HDOwith VGO in 20:80 blending ratio as compared to the processing of pure VGO. They carried out the catalytic cracking reaction in a validated micro-activity test reactor (fixed bed quartz reactor) for VGO cracking over equilibrium FCC catalyst. They further extended the co-processing of HDOwith VGO over various types of FCC catalysts in terms of structural parameters of zeolites [24]. It was mentioned that most of the lignin-derived molecules on co-processing of HDOare partially cracked into smaller methoxyphenols over FCC, HY and HZSM-5 catalysts and reported that very few oxygenated molecules are entered into pores of zeolite.

Mercader et al. [15] carried out the co-processing of HDO with long residue in a fluidized bed MAT-5000 reactor over equilibrium FCC catalyst and reported near normal FCC gasoline (44–46 wt.%) and LCO (23–25 wt.%) products without an excessive increase in undesired coke and dry gases, as compared to the base feed. They further reported that high levels of oxygen can be allowed in upgraded HDO (up to 28 wt.%) for co-processing in FCC unit without deterioration of the yield structure [25]. These studies were further extended for co-processing of catalytic pyrolysis oil (CPO) with VGO and compared the results of co-processing of HDO with VGO [6].

An increase in alkyl phenols in addition to increase in coke, olefins, and aromatics were reported, while co-processing of CPO with VGO as compared to the HDO with VGO. Besides, several researchers [17-19, 27-28] studied the effect of fast pyrolysis oil representative model compounds on product yields while co-processing them with VGO/LCO. However, all these studies are limited to product yields.

Furthermore, The ^{31}P NMR is a powerful analytical technique for identification and quantification of organic oxy-functional groups using derivetization method; it has a unique advantage over ^{1}H and ^{13}C NMR for the measurement of oxy components in biomass. It provides the quantitative information for various types of major hydroxyl groups in a relatively short experimental time with small amounts of sample. Compared to ^{1}H NMR, the large range of chemical shifts reported for the ^{31}P nucleus generates a better separation and resolution of signals. In addition, the 100% natural abundance of the ^{31}P and its high sensitivity renders ^{31}P NMR a rapid analytical tool in comparison with ^{13}C NMR. Among trivalent and pentavalent derivetization agent trivalent phosphorous reagents provides largest chemical shift difference to carry out the identification and quantification. Wroblewski et al. [29] examined five trivalent reagents to derivatize organic model compounds including phenols, aliphatic alcohols, and aromatic and aliphatic acids, with 2 chloro-4,4,5,5-tetramethyl-1,3,2-dioxaphospholane (TMDP). This method may have broad applicability in biomass conversion to second generation bio-fuels [30].

In this perspective, the present investigation discussthe product distribution patterns of FCC on co-processing of VGO with FPO at different blending ratios. The product profile at iso-conversion level catalytic cracking of VGO, VGO with FPO, and VGO with HDO have been compared.HDOHDO Further^{31}P NMR spectroscopic techniques has been employed to

characterize FPO and HDO during pretreatment of feed; while ^{1}H and ^{13}C were used for characterization of products .

2.0 Materials and methods

2.1 Materials

Expelled Jatropha curcas cake (average particle size of ~1.4 mm) was used as a biomass feedstock for fast pyrolysis experiments. Palladium (99.9%, Sigma-Aldrich Chemicals) and γ-alumina Al_2O_3 (97%, Sigma-Aldrich Chemicals) were chosen as an active and support materials for the preparation of hydrodeoxygenating catalyst. The commercially available VGO was used for the co-processing studies, and its characteristics are given inour previous paper [38]. The catalyst used in the advanced cracking evaluation unit was also an industrially available equilibrium fluid catalytic cracking (FCC) catalyst, i.e. E-CAT. The physicochemical characteristics of E–CAT are listed in our previous paper [38]. E-CAT contains synthetic faujacite zeolite (USY or REUSY), silica-alumina matrix, clay (e.g. Kaolin clay) with binder and special additives. The H/C_{eff} of FPO and HDOwere found to be more than the inflection point of 1.2, and are shown in Table 2. Particularly, the feedstock having $H/C_{eff} \geq 1.2$ can be easily processed in fluid catalytic cracking unit for energy production [22].

2.2 HDO catalyst preparation

Mesoporous alumina was prepared using the method proposed by Ray et al. [31]. The Pd was loaded over alumina by incipient wetness impregnation method. In a typical preparation method, 1.0 g of Palladium (II) nitrate dihydrate was dissolved in 30 ml of water, and 20 ml of ethanol. Subsequently, 20 g of γ-alumina (Al_2O_3) (Surface area = 243 m^2 g^{-1}) was added. The mixture

was stirred constantly at 80 °C for 5 hours to dry the sample. The dried sample was further dried at 120 °C for overnight in an oven. Finally, the Pd metal loaded on alumina was calcined at 500 °C in a furnace for 8 h to prepare Pd/Al_2O_3 catalyst (2% Pd on alumina). The typical pore diameter, measured using BET apparatus, of the mesoporous alumina was around 5 nm.

2.3 Fast pyrolysis

The continuous electrically heated bubbling fluidized bed fast pyrolyzer with sand as fluidizing media was used for the fast pyrolysis of biomass at ~530 °C temperature and atmospheric pressure. The fluidizing gas (nitrogen) was preheated up to 400 °C, using an electric furnace. The biomass was fed into the reactor by screw feeder system in continuous mode at a feed rate of 300 g h^{-1}. The char was separated by a cyclone next to the reactor, vapors were condensed and separated as crude fast pyrolysis oil in a series of condensers and the non-condensable gases were vented off to atmosphere. The schematic diagram of fast pyrolysis unit is shown in Figure 1.

2.4 Hydrodeoxygenation

The experiment aimed to produce partially hydrodeoxygenated fast pyrolysis oil, which is suitable for co-processing in petroleum refinery fluid catalytic cracking unit. A known amount (2 wt.%) of palladium on alumina catalyst was used in a 100 ml batch high pressure stirred reactor (USA made autoclave) to hydrogenate the heavy fraction of FPO. Initially, the reactor was purged with hydrogen gas for a period of 5 min, and then it was pressurized up to 80 bar pressure. A constant speed of stirrer was maintained at 700 rpm. The reactor temperature was raised to reaction temperature from ambient with a heating rate of 5 °C min^{-1}. The reaction

temperature was maintained for a period of 4 h. The reactor was then cooled down to ambient temperature. The liquid products were collected and analyzed separately using NMR spectroscopy, and are listed in Table 5. The water content in liquid product was measured with Mitsubishi MCI moisture meter using Karl Fischer technique.

2.5 Catalytic cracking

Advanced Cracking Evaluation (ACE-R^{TM}) unit, M/s. Kayser Technology Texas (USA), was used for catalytic cracking of heavy fraction of fast pyrolysis oil and HDO, which was equipped with an automated fixed-fluidized bed reactor. The schematic diagram of ACE-R unit is shown in Figure 2. A constant amount of catalyst (9 g) was loaded for each experimentand a constant C/O ratio of 5 was maintained by keeping a constant time on-stream (t) of 90 s, feed rate of 1.2 g min^{-1} and weight hourly space velocity (WHSV) of 8 h^{-1}. The reaction was performed at atmospheric pressure and 530 $^{\circ}$C temperature. The catalyst was stripped off by nitrogen for a period of multiple of 7 times of injection time. During the catalytic cracking and stripping steps, the liquid products were collected in a glass receiver, maintained at –10 $^{\circ}$C temperature, which is located at the end of the reactor exit. Meanwhile, the gaseous products were collected in a gas receiver by water displacement method. After cracking and stripping steps the reactor was operated in regeneration mode, where the coke deposited on the catalyst surface during the cracking reaction was burnt off with air at a temperature of 700 °C. The flue gases generated during regeneration process were sent to the catalytic converter/furnace packed with cuprous oxide, where carbon monoxide was converted into carbon dioxide at 540 °C temperature. The step of regeneration process/mode was continued till the amount of carbon dioxide formation is

becomes nil in the flue gases. The reactor effluent gases were measured on-line, which were used to estimate the amount of carbon deposited on E-CAT during cracking (coke).

2.6 Product analysis

The product gases were analyzed with a Varian CP-3800 gas chromatograph equipped with three detectors, a flame ionization detector (FID) and two thermal conductivity detectors. The coke deposited on the catalyst was burned with air in regeneration mode and the resulted total carbon dioxide was analyzed using IR spectroscopy. The liquid products were analyzed by chromatographic simulated procedure described by ASTM D-2887 method with an Agilent 6890 gas chromatograph, using a HP-1 methyl silicon column and a flame ionization detector. As in petroleum refinery practice the product distribution was quantified by their boiling point range: dry gas (H_2 and C_1-C_2 hydrocarbons), LPG (C_3-C_4 hydrocarbons), gasoline (IBP–216 °C), light cycle oil [LCO (216–370 °C)], heavy cycle oil [HCO (> 370 °C)] and coke, respectively. The conversion was estimated using following equation

Conversion, wt.% = 100 – (LCO wt.%+ HCO wt.%) [Scheme I]

For ^{31}P NMR analysis, the solvents used with the bio-oil sample were usually a mixture of anhydrous pyridine and deuterated chloroform (1.6: 1.0, v/v) containing a relaxation agent (i.e., chromium (III) acetylacetonate) and an internal standard. 20 mg of FPO was dissolved in pyridine CDCl3 solvent of 0.5 ml. TMDP reagent (0.05–0.10 ml) was added, stirred and transferred into a 5 mm NMR tube for ^{31}P NMR recording. Quantitative ^{31}P NMR spectra were recorded with a long pulse delay of 10s using a 90^0 ^{31}P pulse. 128 number of transients were recorded in inverse gated decoupling mode on a Bruker Avance III 500 MHz spectrometer at room temperature. Chemical shifts are usually calibrated relative to the phosphitylation product

of TMDP with water (sample moisture), which gives a sharp and stable signal at 132.2 ppm in pyridine-$CDCl_3$ solvent.

^1H and ^{13}C NMR spectra of FCC liquid distillates, produced from co-processing of FPO or HDO with VGO, were recorded on a Bruker Avance III NMR spectrometer equipped with a 5 mm-mm BBFO probe resonating at the frequency of 500.13 and 125.7 MHz, for ^1H and ^{13}C, respectively. The conventional ^1H spectra were recorded using 5% w/v sample solutions in $CDCl_3$ containing 0.03% TMS (99.8% Merck) with a sweep width of 6 kHz, 16 number of scans, 13.4-μs π/2 proton pulse and 2-s relaxation delay. The ^{13}C NMR spectra of the sample were recorded using 30% (w/v) in $CDCl_3$ solutions. Quantitative ^{13}C spectra were acquired using the nuclear overhauser effect (NOE) suppressed, inverse gated proton decoupled technique (Waltz-16), with a sweep width of 19 kHz. 8k numbers of scans were collected using a 5-s relaxation delay. All the ^{13}C spectra were processed with 1.0 Hz line broadening prior to Fourier transform (FT). All the ^1H and ^{13}C NMR spectra were referenced to TMS at 0 ppm. Before starting the analysis, the spectra obtained were corrected for phase and baseline and then each of them was separated into different regions that correspond to different types of protons and carbons according to their position in the molecule. Later, each spectrum was integrated thrice and averaged within the indicated regions.

3.0 Results and discussion

This section has been divided into two parts. In the first part, the discussion is restricted to process, which includes an approach of char removal from the heavy fraction of Jatropha-derived fast pyrolysis oil and hydrodeoxygenation of FPO in order to convert it into HDO over Pd/Al_2O_3 catalyst, (i.e. section 3.1.1). The discussion is further extended to reactions such as co-processing

of FPO with VGO in an ACE-R FCC unit with the blending ratios of 5, 10, 15, 17 and 20%. Furthermore, the product distribution pattern at iso-conversion level of around 66% is discussed in section 3.1.2 for the direct processing of VGO, co-processing of VGO with FPO at 17% blending ratio and co-processing of VGO with HDOat blending ratio of 5%. The second part is highlighted with the discussion on NMR characterization of feed and product (i.e., Section 3.2).

3.1 Process

3.1.1 Pretreatment of fast pyrolysis oil

One of the reasons for the formation of coke on FCC catalyst while co-processing may be the presence of fine char particles which are not completely separated from fast pyrolysis oil. The cyclone separator next to fluidized bed fast pyrolysis reactor is not extremely effective to separate the fine char particles below 2-3 microns [33]. Besides, an ash content of biomass (>1.5%) is enough to maximize the catalytic effect [34] that leads to formation of fine char particles which are difficult to separate with cyclone [35].

Therefore, in the first step of the pretreatment of fast pyrolysis oil, a chemical treatment method has been applied to free the char particles from fast pyrolysis oil. Here, the Jatropha-derived fast pyrolysis oil obtained from bubbling fluidized bed pyrolysis reactor is found to have large concentration of char particles (nano-to-micro scale). Therefore, the heavy fraction of fast pyrolysis oil (in semi-solid form) is diluted with ethanol and then larger size particles (> 200 nm) were separated by membrane filtration under vacuum. Subsequently, the filtrate containing small particles was centrifuged at 8000 rpm for 20 minutes. As a result, the filtrate component was separated into two phases; upper liquid phase containing blend of fast pyrolysis oil and ethanol, and the deposited char particles at the bottom of the centrifuge tubes. The ethanol present in the

residual pyrolysis oil was then recovered by vacuum distillation. After the process, the residual pyrolysis oil is thinner as compared to earlier semi-solid like phase, and which is termed as fast pyrolysis oil (FPO). The FPO was used for further hydrodeoxygenation followed by catalytic cracking.

In the second step of pretreatment of FPO, a hydrodeoxygenation method has been applied to reduce the oxygen content of FPO. The obtained FPO, containing 32 wt.% of oxygen, was subjected to hydrodeoxygenation with Pd/Al_2O_3 catalyst in a batch stirred reactor at 80 bar pressure. The increase of reactor pressure from 80 to 105 and 120 bars was observed with increase in temperature from ambient to 250 and 300 $^{\circ}$C, respectively. The gas analysis indicated that the bound oxygen was removed in the form of carbon dioxide by decarboxylation reaction, which is higher in yield, i.e. 45 and 51 wt.%, at 250 and 300 $^{\circ}$C temperatures, respectively. The respective CHNO elemental analysis of feed Jatropha curcas cake, FPO and HDO are shown in Table 1. From the elemental analysis (Table 1), it was found that the amount of oxygen content is reduced from 32 to 22 and 10 wt.% for 250 and 300 $^{\circ}$C temperatures, respectively. If the oxygen contents could not be removed, the deep or high deoxygenation levels of >95% is needed to match the specifications of pyrolysis oil with standard crude oil in terms of carbon-hydrogen ratio, oxygen content and density [10]. The Van krevelen diagram for dry H/C and O/C ratios of the FPO and HDOis shown in Figure 3. The O/C atomic ratio of HDO is drastically decreased to 0.257 and 0.099, respectively, as compared to FPO (0.424); whereas a relatively minor change and declination in H/C ratio at 250 $^{\circ}$C and 300 $^{\circ}$C temperature, respectively was observed. A similar kind of trend was observed by Mercader et al. [36]. From CCR analysis (Table 2), the carbon residue was found to be higher (~16 wt.%) in FPO; whereas it is decreases to ~about 8 wt.% on hydrodeoxygenation at 300 $^{\circ}$C temperature.

3.1.2 Co-processing of FPO/HDO with VGO

The catalytic cracking studies on co-processing of FPO with VGO was carried out in a advanced cracking evaluation (ACE–R) FCC unit at the optimum operating conditions. The operating parameters were decided on the basis of results obtained from the catalytic cracking of pureVGO in FCC unit at different temperature and C/O ratios, which are mentioned in our previous publication [32]. The maximum yield of gasoline was found to be 44 wt.% at C/O ratio of 5 and 530 °C temperature with the FCC conversion of ~66%. The similar kind of optimized process parameters were used for further co-processing reactions of VGO with FPO/HDO.

Initially the blending ratio of FPO with VGO was varied at 5, 10, 15, 17, and 20% in order to see its effect and optimize the same for getting the simillar FCC conversion. The FCC conversion of different feeds and their product yields of dry gas, LPG, gasoline, LCO, HCO, and coke are shown in Table 3. The mass balance obtained was more than 98%. From Table 3 it can be seen that the conversion decreases from 75 to 64 % with an increase in blending ratio of FPO from 5 to 20%. The decrease in conversion is due to the decrease in yield of dry gases and LPGfrom 2.1 to 1.4 and 38 to 23 wt.%, respectively. Whereas, the yields of gasoline, LCO and HCO were increased from 29 to 35 wt.%, 14 to 20 wt.%, and 8 to 14 wt.%, respectively, with an increase in blending ratio of the FPO with VGO from 5:95 to 20:80. However, the results of co-processing at a lower blending ratio (5:95) indicated higher conversion (~around 9 wt.%) as compared to the direct catalytic cracking of pure VGO at constant C/O ratio and temperature. It was due to higher yield (38 wt.%) of LPG fraction as compared to 15 wt.% in case of catalytic cracking of pure VGO. The increase in LPG yield was observed at the cost of gasoline yield, which was 29 wt.%; while the gasoline yield obtained from the catalytic cracking of pure VGO was 44 wt.%.. Further, there was also a decrease in LCO and HCO yields by 5 and 4 wt.%, respectively.

However, with increase in blending ratio from 5:95 to 10:90, there was decrease in the LPG yield by ~3 wt.%; increase in gasoline yield by ~2 wt.%; increase in LCO yield by ~1 wt.%; and a slight increase in HCO yield by ~0.5%. Clearly these results indicated that the FPO could be co-processed with VGO at lower blending ratios of 5:95 and 10:90 for LPG production at the cost of gasoline followed by LCO and HCO range hydrocarbons.

Further, with increase in blending ratio from 10:90 to 15:85, a similar (as 10:90 blending studies) trend of LPG (decreases by 7 wt.%), gasoline (increases by 4 wt.%), LCO (increases by 2.5 wt.%), HCO (increases by 2 wt.%) yields were observed. Moreover, with an increase in blending ratio FPO:VGO to 17% the FCC conversion of ~66% was observed. At this particular blending ratio, the dry gas, gasoline, and coke yields were lowered by 0.4, 9, and 1.4 wt.%, respectively; whereas the yield of LPG was increased by ~10 wt.% and the yields of LCO and HCO were found to be almost constant.

The similar trend of product yields were observed with an increase in blending ratio from 17:83 to 20:80. In general perspective, C5+ liquid hydrocarbons increases with an increase in H/C_{eff}, and similar observations were made in the present study. There was a decrease in C5+ hydrocarbons with an increase in H/C_{eff}. From the above results, it is also believed that in addition to H/C_{eff} the type of oxygenated molecules present in FPO also plays a major role in the distribution of FCC product profile. However, the increase in the yield of gasoline with increase in blending ratio of FPO with VGO is observed even with the decrease in H/C_{eff} . This was due to the presence of lignin monomers in the FPO, and the same is discussed with the help of NMR analysis in the following section.

The coke yield for all blending ratios is within the limits and is lower as compared to pure VGO processing. The previous studies on co-processing of aliphatic oxygenates like acetic acid, hydroxyacetone and glycolaldehyde with VGO for similar conditions also indicated the coke yield within the limits except on co-processing of lignin-derived monomer (guaiacol) with VGO [32, 38].Wwater formation was also observed on co-processing of FPO with VGO; however their yield is not shown.

Furthermore, an attempt has been made to co-process the HDO, obtained on hydrodeoxygenation of FPO at 300 °C temperature and 80 bar pressure, with VGO in a blending ratio of 5:95 in an ACE-R unit. The conversion was found to be 66.96%, which is approximately equilent to the conversion obtained oncatalytic cracking pure VGO or co-processing of FPO with VGO for similar operating parameters. It shows that the highest conversion is possible with co-processing of HDO with VGO as compared to pure VGO catalytic cracking and co-processing of FPO with VGO. The increase in conversion is due to the increase in the yields of LPG and gasoline. However,and the yields of LCO and HCO were observed in similar for all cases.. The increase in the effective hydrogen index from 1.65 to 1.68 on addition HDO instead of FPO resulted in an increase in the yield of C5+ liquid hydrocarbons. HDO

3.2 NMR characterization

3.2.1 Hydrodeoxygenation of FPO

^{31}P NMR has been employed for characterizing hydroxyls by phosphitylation with a phosphorous reagent followed by quantitative ^{31}P analysis [37]. The oxygenates in the fast pyrolysis oil are problematic components aroused from the cracking of ligno-cellulosic

components of biomass, and imposed complexity in ^{1}H NMR analysis, and takes long time for ^{13}C measurement due to long relaxation time of C-O groups. ^{31}P derivatization is a preferred method for fast analysis of oxy-component in pyrolysis oil. Thus, the oxygenates like aliphatic and aromatic alcohols, and acids were derivatized using TMDP and quantified from ^{31}P spectra. The reaction scheme for phosphorous derivatization is shown in Figure 4. TMDP reacts with hydroxyl groups in the presence of a base such as pyridine to form phoshitylated product, with the base to capture the liberated HCl and drive the exothermic reaction to complete conversion. All the oxy-components are derivatized and the typical chemical shift assignment with integration regions are tabulated for different hydroxyl groups in Table 4. ^{31}P NMR spectra of derivatized FPO and HDO (at 250 and 300 °C) are shown in Figure 5. The chemical shifts are referenced with respect to the internal standard NHND (152 ppm). Carboxylic acids corresponding to chemical shift region of 133-136 ppm are found to be absent in FPO, as shown in Figure 5a. The above result is also evidenced from ^{13}C NMR results showing absence of carboxylic carbon peaks. It is clearly observed from the spectra that the aliphatic alcohols corresponding to chemical shift regions of 145.07 to 150.02 ppm are present in FPO while absent in HDO (300 $^{\circ}$C). It indicated the reduction in hydroxyl groups due to process conditions and the process is efficient for hydrodeoxygenation. The FPO contains a major guaiacyl phenolic, and p-hydroxy phenyl phenolics. Although from the Figure 5b it can be seen that the signals due to phenols and syringyl alcohols corresponding to region 142-144 ppm are present in HDO (obtained at 250 °C); whereas Figure 5c shows that the components are completely removed in HDO (obtained at 300 °C). Moreover, strong signals due to guaiacol, catechol and p-hydroxy phenyl groups are completely removed in HDO (obtained at 300 °C). On the basis of ^{31}P NMR analysis, it was found that hydroxyl and mono lignol groups were eliminated during

hydrodeoxygenation. Thus, the HDO obtained at 300 °C can be used along with VGO as a co-processing feedstock for processing in a refinery FCC unit. The HDO obtained, at 300 °C temperature, was used for further co-processing studies.

3.2.2 Co-processing of FPO/HDO with VGO

The average structural parameters of FCC product liquid distillates were studied using NMR spectroscopy. The chemical shift region of ^{1}H spectrum has been subdivided into aromatic hydrogen (9-6 ppm), aliphatic hydrogen (0-5 ppm), olefinic (5-6) and oxygeneted hydrogen (3.5-5 ppm), as shown in Figures 6a–6c. The aliphatic proton region has been further subdivided into Hα (2-3 ppm), Hβ (1-2 ppm), Hγ regions (0.5-1 ppm) [2-3]. Further, the aromatic region has been divided into mono aromatics (m-a; 6-7.2ppm), diaromatic (d-a; 7.2-8.00 ppm) and polyaromatic proton regions (p-a; 8-10ppm). The ^{13}C NMR spectrum has been divided into different integration domains as aliphatic (0-50 ppm), oxygenated alcoholic (50-110 ppm), aromatic (110-150 ppm) and carboxylic (150-200) carbons (Figures 6d–6e). Figures 7a-7e and Figure 8a-8e represents ^{1}H NMR and ^{13}C NMR spectra of the blended VGO. From the normalized integrals of the signals, a series of average structural parameters like average chain length (n), fraction of carbon aromaticity (f_a), percentage of proton aromatic carbon (Ch), bridgehead aromatic carbon (Cb), substituted aromatic carbon (ARq), branchiness Index (BI), fraction of substituted aromatics (f_a^s, percentage of mono-aromatics (m-a), di-aromatics (d-a), and poly-aromatics (p-a) protons have been derived and are listed in Table 5. The results can only be considered approximate, since they present an over-simplified picture of very complex mixtures containing a wide range of components; however the method described has the advantage that the few spectra can be obtained on crude material without preliminary treatment. Table 5 shows the average structural parameters of VGO, and blended VGO and their products.

The average alkyl chain length of VGO is 18 while in the products the average chain length varies from 3-6. The fraction of carbon aromaticity varies from 0.13 in VGO to the range of 0.13-0.14 in FPO blended VGO and to 0.15 in HDO. In products, the aromaticity varies from 0.47 to 0.55. From Table 5 it can be seen that on addition of FPO with VGO results into increase in f_a. This indicates the incomplete cracking of lignin-derived monomers which are present in FPO; whereas, the co-processing of HDO (obtained at 300 °C) with VGO resulted into a product with a similar f_a of ~0.47, which indicates that the lignin-derived monomers are cracked with hydrodeoxygenation of FPO. This is also confirmed from the yield of gasoline on co-processing of HDO with VGO, which is higher while co-processing of FPO with VGO. HDOAgain the total CH_3 carbon content remains same and the amount of long end chain CH_3 is lower in the case of co-processing of FPO (at 5:95 ratio) as compared to the co-processing of HDO (at 5:95 ratio). The finding is also reflected from higher value of branchiness index (BI) in oil (at 5:95). This indicates that the product of HDO co-processing with VGO contain more iso-paraffinic CH_3 substructure and the product of FPO co-processing with VGO contains more paraffinic CH_3 substructure. Further, the fraction of substituted aromatics fa^s shows the fraction of aromatics substituted per molecule. In the feeds H/C_{eff} is found to vary from 1.47 to 1.725. The aromatic protons vary from 15.5 to 21.69, with higher di-aromatic and poly aromatic protons in products for blending ratios of 5:95 and 10:90. This indicates that the product of HDO co-processing with VGO contain more paraffinic CH_3 substructure and the product of FPO co-processing with VGO contains more iso-paraffinic CH_3 substructure. Further, the normalized average percentage of protonated aromatic carbons varies from 37.2 to 44.2, bridgehead aromatic carbons varies from 2.9 to 3.3, substituted aromatics varies from 6.3 to 7.8. The branchiness index shows the percentage of branching within the alkyl side chains. Higher the BI, more is the branched side

chains to aromatics. The Table 5 also shows that the side chains are more branched in the blending ratio of 20:80.

4.0 Conclusion

The petroleum-derived pure VGO and mixtures of the heavy fraction of Jatropha curcas cake-derived fast pyrolysis oil and its HDO with VGO were used as the feedstocks for the present co-processing studies. The FPO containing 32 wt.% of oxygen seems to be not suitable for co-processing with petroleum-derived VGO at optimized process conditions of FCC unit for higher gasoline as the FPO containing the lignin-derived monomers along with it and which cannot be cracked with FCC catalysts. However, the lower blending ratios of 5:95 and 10:90 of FPO with VGO is very much suitable for the production of light olefins mainly LPG at the loss of gasoline range hydrocarbons. Whereas the decrease in dry gas yield and increase in liquid hydrocarbons were observed with an increase in the FPO blending ratio with VGO. The hydrodeoxygenating Pd/Al_2O_3 catalyst was seems to be very effective in order to reduce the oxygen content of FPO from 32 to 10 wt.% at the lower operating pressure of 80 bar and 300 °C temperature. On co-processing of HDO with VGO resulted in an increase in the yields of gasoline and LCO as compared to the co-processing of FPO with VGO, at the similar blending ratio of 5:95. The FCC distillate on co-processing of FPO with VGO is containing more iso-paraffinic CH_3 substructure components; whereas the liquid on co-processing HDO with VGO is containing more paraffinic CH_3 substructure. The coke yield was found to be within the limit and in fact lower than the pure VGO processing over the same equilibrium FCC catalyst. Based on the results of present experimental investigations, it may be inferred to co-process the HDO instead of FPO with VGO

at lower blending ratio of up to 5:95 in FCC unit without many modifications in the process configuration and catalyst if demand of LPG is more, as is the case in India.

Acknowledgements

The authors express sincere thanks to Mr. Shiv Prasad Nautiyal of CSIR-Indian Institute of Petroleum for his unconditional support/participation in continuous operation of biomass fast pyrolysis unit. Further authors extend their thankfulness to FCC group of CSIR-IIP for allowing us to carry out the catalytic cracking studies in ACE-R unit.

Abbreviations

LPG	Liquefied petroleum gas
LCO	Light cycle oil
HCO	Heavy cycle oil
FPO	Heavy fraction of Jatropha-derived char free fast pyrolysis oil
H/C_{eff}	Effective hydrogen index based on elemental analysis
C/O	Catalyst-to-oil ratio
n	Average chain length
f_a	Fraction of aromaticity
Ch	Protonated aromatic carbon
Cb	Bridgehead aromatic carbon

ARq	Substituted aromatic carbon
BI	Branchiness Index
f_a^s	fraction of substituted aromatics
m-a	Mono-aromatic protons
d-a	Di-aromatic protons
p-a	Poly-aromatic protons
ab	absent
H/C	Hydrogen-to-carbon atomic ratio
O/C	Oxygen-to-carbon atomic ratio
E-CAT	Equilibrium FCC catalyst
IBP	Initial boiling point, °C
FBP	Final boiling point, °C
CCR	Conradson carbon residue, wt.%

References

1. C. John, H. Paul, J.A. Beamon, S. Naolitano, A.M. Schaal, J.T. Turnure, and L.Westfall, *International Energy Outlook 2013*, 2013, Report number: DOE/EIA-0484 (2013).
2. Worldwide look at reserves and production, *Oil & Gas Journal*, 2012, **110**, 28-31, http://www.ogj.com (subscription site).

3. D.C. Elliott, and E.G. Baker, Upgrading biomass liquefaction products through hydrodeoxygenation, *Biotech. Bioeng. Symp.*, 1984, **14**, 159–174.
4. D.C. Elliott, and G.F. Schiefelbein, Liquidhydrocarbon fuels from biomass, Abstracts of papers of the *American Chemical Society*, 1989, **34**, 1160–1166.
5. A. Demirbas, Biorefineries: For biomass upgrading facilities. *Green Energy and Technol.*, 2010, 75-92.
6. Approach to refining processes, http://petrofed.winwinhosting.net/upload/25-28May10/S_Bose.pdf (accessed on 23rd May, 2014).
7. G.W. Huber, and A. Corma, Synergies between Bio- and Oil Refineries for the Production of Fuels from Biomass, *Angew. Chem. Int. Ed.,* 2007, **46**, 7184–7201.
8. R.H. Venderbosch, A.R. Ardiyanti, J. Wildschut, A. Oasmaa, and H.J. Heeres, Stabilization of biomass-derived pyrolysis oils, 2010, http://onlinelibrary.wiley.com/doi/10.1002/jctb.2354/pdf, (accessed on 23rd May, 2014).
9. F.M. Mercader, M.J. Groeneveld, S.R.A. Kersten, R.H. Venderbosch, and J.A. Hogendoorn, Pyrolysis oil upgrading by high pressure thermal treatment, *Fuel,* 2010, **89**, 2829–2837.
10. M.C. Samolada, W. Baldauf, and I.A. Vasalos, Production of a bio-gasoline by upgrading biomass flash pyrolysis liquids via hydrogen processing and catalytic cracking, *Fuel,* 1998, **77**, 1667–1675.
11. J. Wildschut, F.H. Mahfud, R.H. Venderbosch, and H.J. Heeres, Hydrotreatment of Fast Pyrolysis Oil Using Heterogeneous Noble-Metal Catalysts, *Ind. Eng. Chem. Res.,* 2009, **48**, 10324–10334.
12. E. Churin, P. Grange, and B. Delmon, Quality Improvement of Pyrolysis Oils, Report number: EUR 12441 EN, Commission of the European Communities, 1989.

13. R.J. French, J. Stunkel, and R.M. Baldwin, Mild Hydrotreating of Bio-Oil: Effect of Reaction Severity and Fate of Oxygenated Species, *Energy Fuels,* 2011, **25**, 3266–3274.

14. P. Grange, E. Laurent, R. Maggi, A. Centeno, and B. Delmon, Hydrotreatment of pyrolysis oils from biomass: reactivity of the various categories of oxygenated compounds and preliminary techno-economical study, *Catal. Today,* 1996, **29**, 297-301.

15. F.M. Mercader, M.J. Groeneveld, S.R.A. Kersten, N.W.J. Way, C.J. Schaverien, J.A. Hogendoorn, Production of advanced biofuels: Co -processing of upgraded pyrolysis oil in standard refinery units, *Appl. Catal., B,* 2010, **96**, 57-66.

16. P.A. Zapata, J. Faria, M.P. Ruiz, D.E. Resasco, Condensation/Hydrogenation of Biomass-Derived Oxygenates in Water/Oil Emulsions Stabilized by Nanohybrid Catalysts, *Top. Catal.,* 2012, **55**, 38–52.

17. I. Graça, F.R. Ribeiro, H.S. Cerqueira, Y.L. Lam, M.B.B. de Almeida¸ Catalytic cracking of mixtures of model bio-oil compounds and gasoil, *Appl. Catal., B,,* 2009, **90**, 556–563.

18. A. Corma, G.W. Huber, L. Sauvanaud, and P.O. Connor, Processing biomass-derived oxygenates in the oil refinery: Catalytic cracking (FCC) reaction pathways and role of catalyst, *J. Catal.,* 2007, **247**, 307–327.

19. G. Fogassy, N. Thegarid, G. Toussaint, A.C. Van veen, Y. Schuurman, and C. Mirodatos, Biomass derived feedstock co-processing with vacuum gas oil for second-generation fuel production in FCC units, *Appl. Catal., B,* 2010, **96**, 476–485.

20. S.B. Jones, J.E. Holladay, C. Valkenburg, D.J. Stevens, C.W. Walton, C. Kinchin, D.C. Elliott, and S. Czernik, Production of Gasoline and Diesel from Biomass via Fast Pyrolysis, Hydrotreating and Hydrocracking: A Design Case, PNNL Report No-18284, US Department of Energy, February 2009.

21. M.S. Talmadge, R.M. Baldwin, M.J. Biddy, R.L. McCormick, G.T. Beckham, G.A. Ferguson, S. Czernik, K.A. Magrini-Bair, T.D. Foust, P.D. Metelski, C. Hetrick, and M.R. Nimlos, A perspective on oxygenated species in the refinery integration of pyrolysis oil, *Green Chem.*, 2014, **16**, 407-453.

22. N.Y. Chen, J.T.F. Degnan, and L.R. Koenig, Liquid Fuel from Carbohydrates. *Chem. Tech.,* 1986, **16**, 506-511.

23. G. Fogassy, N. Thegarid, G. Toussaint, A. C. van Veen, Y. Schuurman, and C. Mirodatos, Biomass derived feedstock co-processing with vacuum gas oil for second-generation fuel production in FCC units, *Appl. Catal., B,* 2010, **96**, 476–485.

24. G. Fogassy, N. Thegarid, Y. Schuurman, and C. Mirodatos, From biomass to bio-gasoline by FCC co-processing: effect of feed composition and catalyst structure on product quality, *Energy Environ. Sci.*, 2011, **4**, 5068-5076.

25. F.M. Mercader, Pyrolysis oil upgrading for co-processing in standard refinery units, Ph.D. Thesis, University of Twente, Netherlands, 2010.

26. N. Thegarid, G. Fogassy, Y. Schuurman, C. Mirodatos, S. Stefanidis, E.F. Iliopoulou, K. Kalogiannis, and A.A. Lappas, Second-generation biofuels by co-processing catalytic pyrolysis oil in FCC units, *Appl. Catal., B,* 2013, **145**, 161-166.

27. I. Graça, J.M. Lopes, M.F. Ribeiro, F.R. Ribeiro, H.S. Cerqueira, and M.B.B. de Almeida, Catalytic cracking in the presence of guaiacol, *Appl. Catal., B,* 2011,**101**, 613–621.

28. A.A. Lappas, S. Bezergianni, and I.A. Vasalos, Production of biofuels via co-processing in conventional refining processes, *Catal. Today,* 2009, **145**, 55–62.

29. A.E.Wroblewski, C. Lensink , R. Markuszewski , and J. G, Verkade. Phosphorus-31 NMR spectroscopic analysis of coal pyrolysis condensates and extracts for heteroatom functionalities possessing labile hydrogen, *Energy Fuels*, 1988, **2**, 765–774.

30. A. Majhi, Y.K. Sharma, R. Bal, B. Behera, and J. Kumar, Upgrading of Bio-oils over PdO/Al_2O_3 Catalyst and Fractionation, *Fuel*, 2013, **107**, 131-137.

31. J. C. Ray, Kwang-Seok You, Ji-Whan Ahn, and Wha-Seung Ahn. Mesoporous alumina (I): Comparison of synthesis schemes using anionic, cationic, and non-ionic surfactants. *Micropo. Mesopo. Mat.*, 2007, **100**, 183–190.

32. D.V. Naik, V. Kumar, B. Prasad, B. Behera, N. Atheya, K.K. Singh, D.K. Adhikari, and M.O. Garg, Catalytic cracking of pyrolysis oil oxygenates (aliphatic and aromatic) with vacuum gas oil and their characterization, *Chem. Eng. Res. Des.*, 2013, **DOI**: 10.1016/ j.cherd.2013.12.005.

33. M. Ringer, V. Putsche, and J. Scahill, Large-Scale Pyrolysis Oil Production: A Technology Assessment and Economic Analysis. *National Renewable Energy Laboratory Technical Report,* NREL/TP-510-37779, November 2006.

34. F.A. Agblevor, S. Besler, A. E. Wiselogel, Fast Pyrolysis of Stored Biomass Feedstocks, *Energy Fuels*, 1995, **4**, 635-640.

35. K. Raveendran, A. Ganesh, and C. K. Kartic, Influence of mineral matter on biomass pyrolysis characteristics, *Fuel*, 1995, **12**, 1812-1822.

36. F.M. Mercader, M.J. Groeneveld, S. R. A. Kersten, C. Geantet, G.Toussaint, N.W. J. Way, C.J. Schaverien, K.J.A. Hogendoorn, Hydrodeoxygenation of pyrolysis oil fractions: process understanding and quality assessment through co-processing in refinery units, *Energy Environ. Sci.,* 2011, **4**, 985-997.

37. Y. Pu, S.Cao, A.J. Ragauskas, Application of quantitative ^{31}P NMR in biomass lignin and biofuel precursors Characterization, *Energy Environ. Sci.,* 2011, **4**, 3154-3166.

38. D.V. Naik, V. Kumar, B. Prasad, B. Behera, N. Atheya, D.K. Adhikari, K.D.P.Nigam, and M.O. Garg, Catalytic cracking of C2-C3 carbonyls with vacuum gas oil, *Ind. Eng. Chem. Res.,* 2014, **DOI:** 10.1021/ie501331b.

List of Tables

List of Figures

Table 1: Elemental analysis of Jatropha cake, fast pyrolysis oil and HDO

Sample name	C, wt.%	H, wt.%	N, wt.%	O, wt.%	S, wt.%	H/C	O/C
Jatropha curcas cake	45.50	6.70	2.43	45.33	0.04	1.767	0.747
Fast pyrolysis oil	56.50	7.10	4.308	32.0	0.092	1.507	0.424
HDO at 250 $^{\circ}$C	64.98	8.0	4.91	22.0	0.11	1.500	0.257
HDO at 300 $^{\circ}$C	76.18	8.8	4.91	10.0	0.11	1.404	0.099

Table 2: Physico-chemical characterization and SIMDIST analysis of feedstock.

Feedstock	Blending ratio	Density at 15 °C, g cc^{-1}	CCR, wt.%	H/C$_{eff}$	Boiling point range, °C							
					Mass recovery, wt.%	IBP	10 %	30%	50%	70%	90%	FBP
VGO	100	0.919	3.64	1.725		350	369	400	441	489	550	550
FPO	100	1.18	16.26	--		36	162	259	328	357	445	592
VGO:FPO	95:5	0.932	4.27	1.65		36	359	393	435	482	545	592
	90:10	0.945	4.90	1.59		36	348	386	430	476	539	592
	85:15	0.958	5.53	1.53		36	337	379	424	469	534	592
	80:20	0.971	6.16	1.47		36	327	372	418	462	529	592
HDO	100	1.04	8.6	--		36	159	270	344	405	499	597
VGO:HDO	95:5	0.925	3.88	1.68		36	358	394	436	485	548	597

Table 3: A selectivity data of for VGO:FPO, VGO:HDO and pure VGO at different blending ratios.

Feedstock's	VGO:FPO				VGO:HDO	VGO	VGO:FPO
Blending ratio	95:5	90:10	85:15	80:20	95:5	100	83:17
FCC conversion	75.68	74.69	69.35	64.39	66.96	66.89	66.08
				Yield, wt.%			
Dry gas	2.182	2.05	1.43	1.41	1.507	1.798	1.42
LPG	38.876	35.70	28.69	23.77	28.78	15.5	25.44
Gasoline	29.038	31.14	35.11	35.04	32.50	44.02	35.08
LCO	14.885	15.43	17.99	20.49	18.98	19.84	19.11
HCO	8.054	8.48	10.67	14.08	13.27	12.4	12.31
Coke	5.48	5.21	4.23	4.16	4.17	5.58	4.14

Table 4: Hydroxyl group contents of FPO and HDO determined by quantitative ^{31}P NMR after derivatization with 2-chloro-4, 4, 5, 5-tetramethyl-1, 3, 2-dioxaphospholane (TMDP)

Sr. No.	Functional group	Integration region, ppm		FPO	HDO, 250 °C	HDO, 300 °C
		Ben et al. [9]	Present study			
1	Aliphatic OH	150.0 to 145.5	150.02 to 145.07	2.37	0.27	ab
2	C5 substituted β-5	144.7 to 142.8	145.07 to 140.42	1.23	0.6	ab
3	Guaiacyl phenolic OH	140.0 to 139.0	140.42 to 138.2	6.2	1.51	ab
4	p-hydroxy-phenyl OH	138.2 to 137.3	138.2 to 136.96	5.75	1.89	ab

Table 5: NMR derived average structural parameters of feedstock's and their liquid distillates (denoted with*) at constant C/O ratio of 5.

Feedstock	Blending Ratio	n	fa	Ch	Cb	ARq	BI	fa^s	m-a	d-a	p-a
VGO	100	18	0.13	4.90	1.36	5.70	0.35	0.44	2.33	1.6	0.55
VGO*		6	0.48	37.27	3.19	7.32	--	0.15	9.2	7.63	2.15
FPO:VGO	5:95		0.13								
FPO:VGO*		3	0.55	43.5	3.3	7.8	0.47	0.14	10.56	8.66	2.47
FPO:VGO	10:90		0.13								
FPO:VGO*		3	0.54	44.2	3.1	6.4	0.53	0.12	10.00	8.51	2.58
FPO:VGO	15:85		0.14								
FPO:VGO*		3	0.52	41.7	3.0	6.8	0.47	0.13	10.46	6.84	1.05
FPO:VGO	20:80		0.14								
FPO:VGO*		3	0.49	39.5	2.9	6.7	0.6	0.14	10.05	5.26	0.19
HDO: VGO	5:95		0.15								
HDO:VGO*		3	0.47	37.2	3.0	6.3	0.53	0.13	9.67	5.51	0.79

Graphical abstract

Co-processed the jatropha-derived heavy or tar fraction of fast pyrolysis oil (FPO) and hydrodeoxygenated fast pyrolysis oil (HDO) with VGO in an advanced cracking evaluation fluid catalytic cracking (FCC) unit. Also oxy–components in fast pyrolysis oil and hydrodexogenated oils are analyzed using ^{31}P NMR.

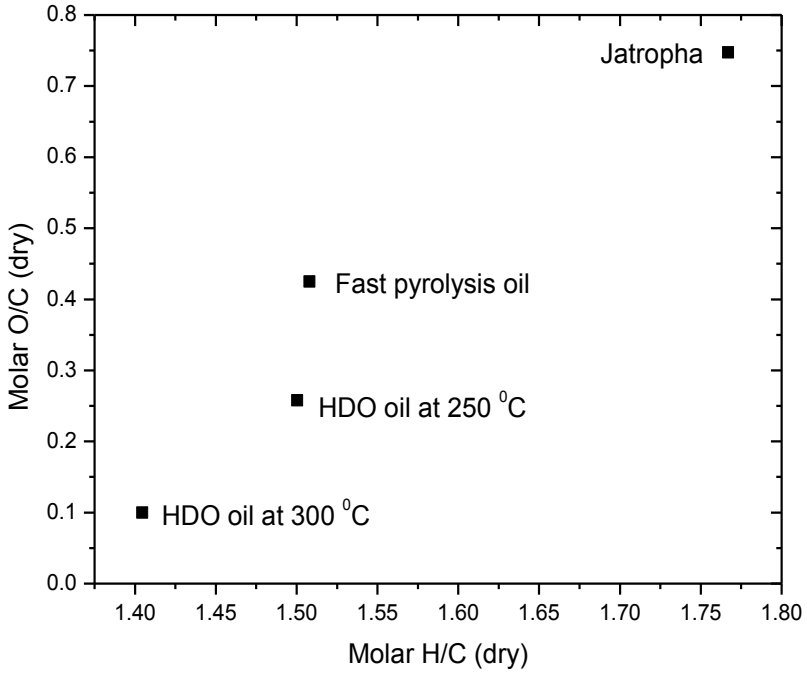

Van Krevelen diagram for dry H/C and O/C ratios of the FPO and HDO oils

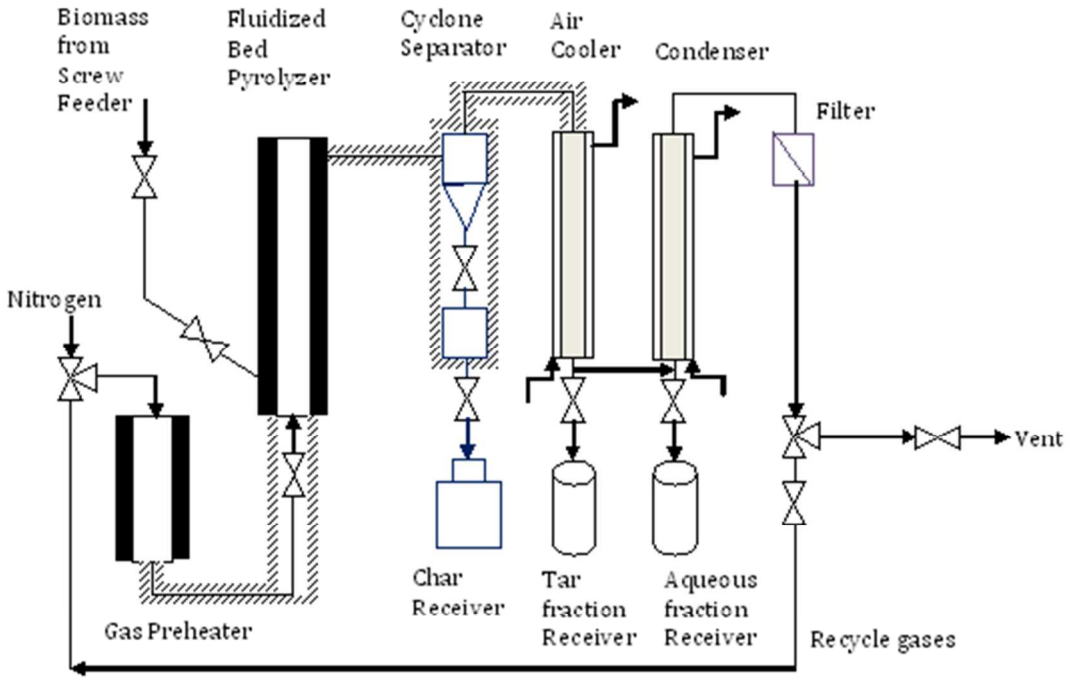

Figure 1: Schematic diagram of bubbling fluidized bed fast pyrolyzer.

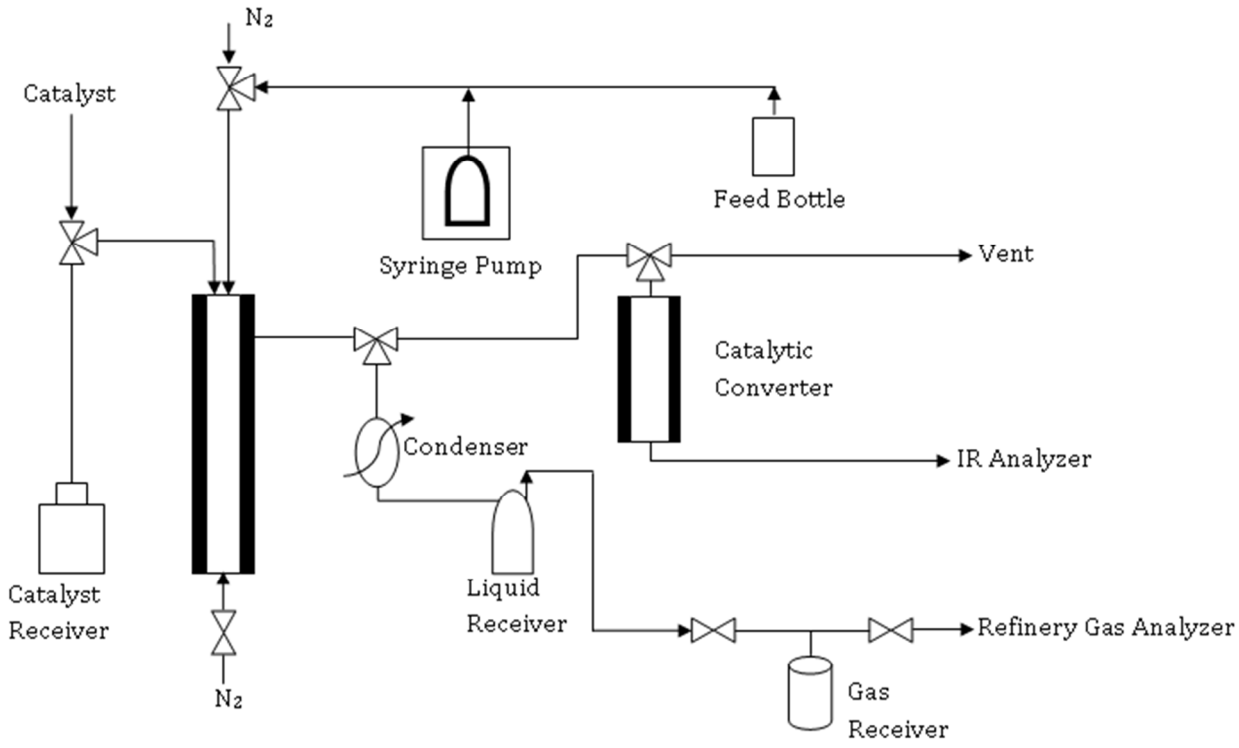

Figure 2: Schematic diagram of advanced cracking evaluation (ACE-R) FCC unit.

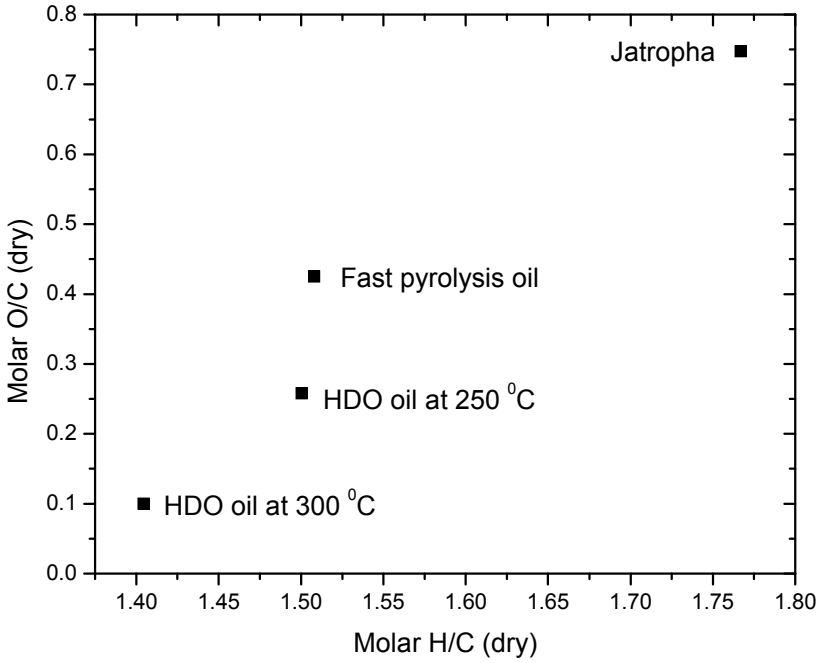

Figure 3: Van Krevelen diagram for dry H/C and O/C ratios of the FPO and HDO.

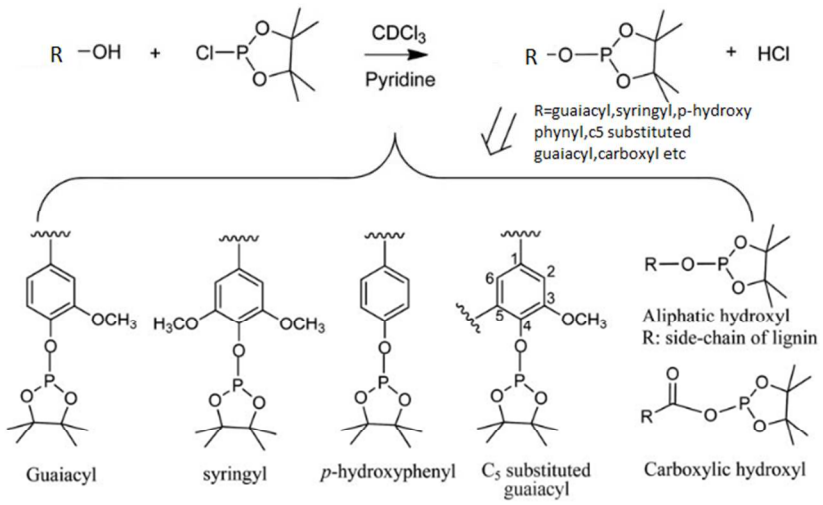

Figure 4: A reaction scheme for phosphitylation of hydroxyl groups of lignin structural units with TMDP

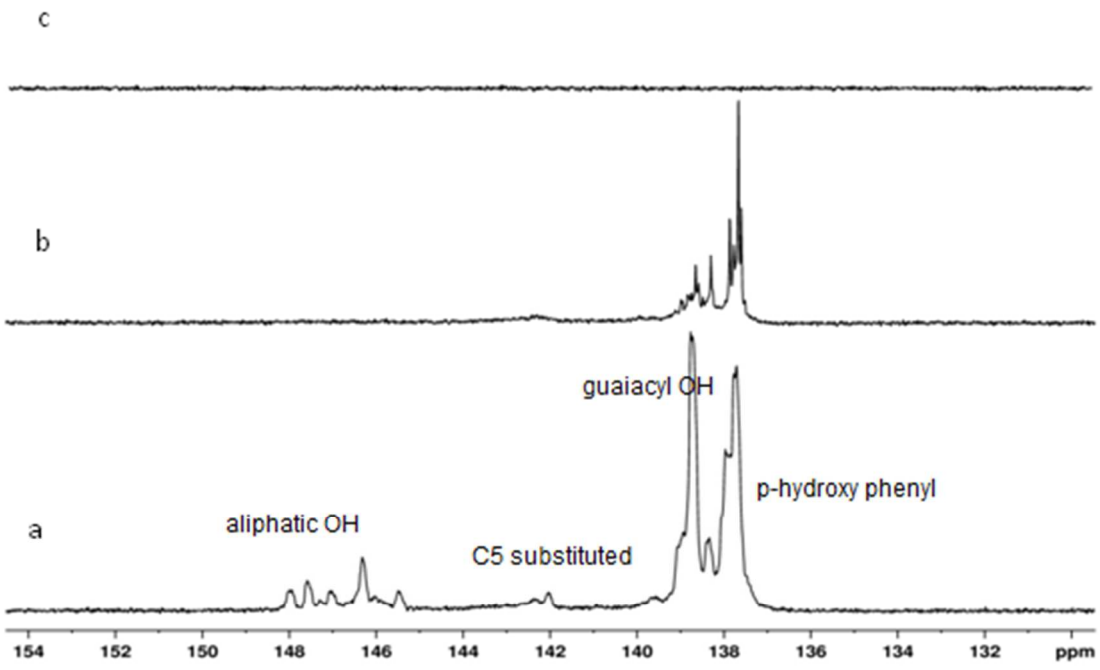

Figure 5: Quantitative ^{31}P NMR of (a) FPO; (b) HDO oil at 250 °C; and (c) HDO oil at 300 °C.

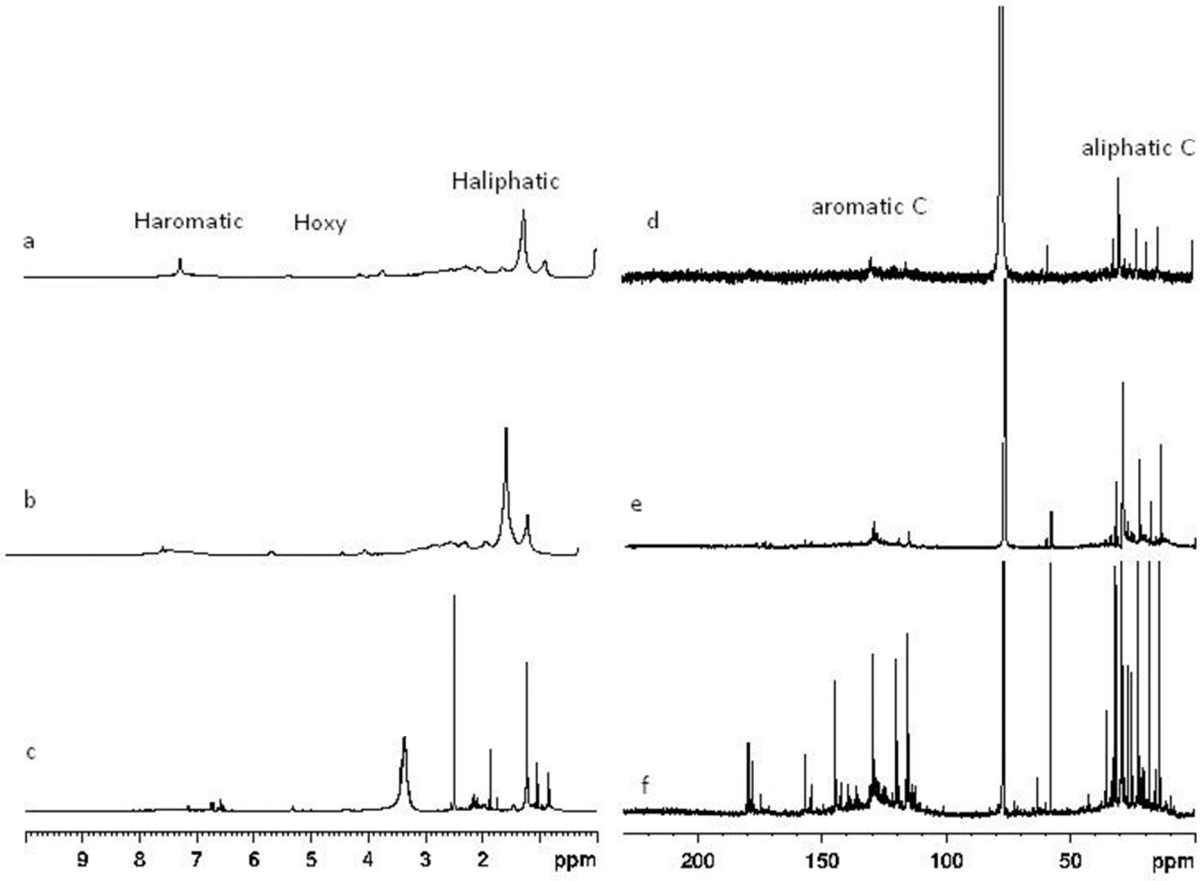

Figure 6: (a) ^{1}H of HDO oil at 300 °C; (b) ^{1}H of HDO oil at 250 °C; (c) ^{1}H of FPO; (d) ^{13}C NMR of HDO oil at 300 °C; (e) ^{13}C NMR of HDO oil at 250 °C; (f) ^{13}C NMR of FPO.

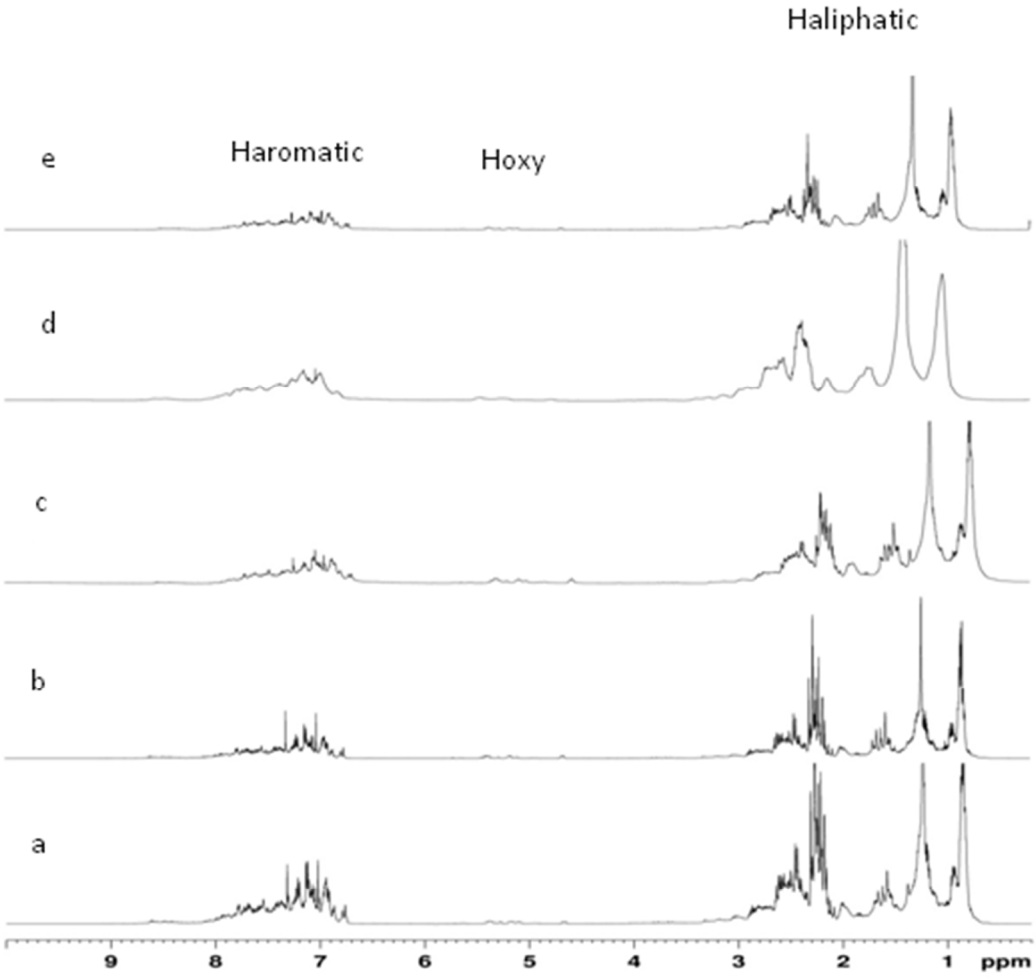

Figure 7: ^{1}H NMR of FCC liquid distillates on co-processing of FPO with VGO in a blending ratio of (a) 5:95; (b) 10:90; (c) 15:85; (d) 20:80 and (e) co-processing of HDO oil with VGO in a blending ratio of 5:95

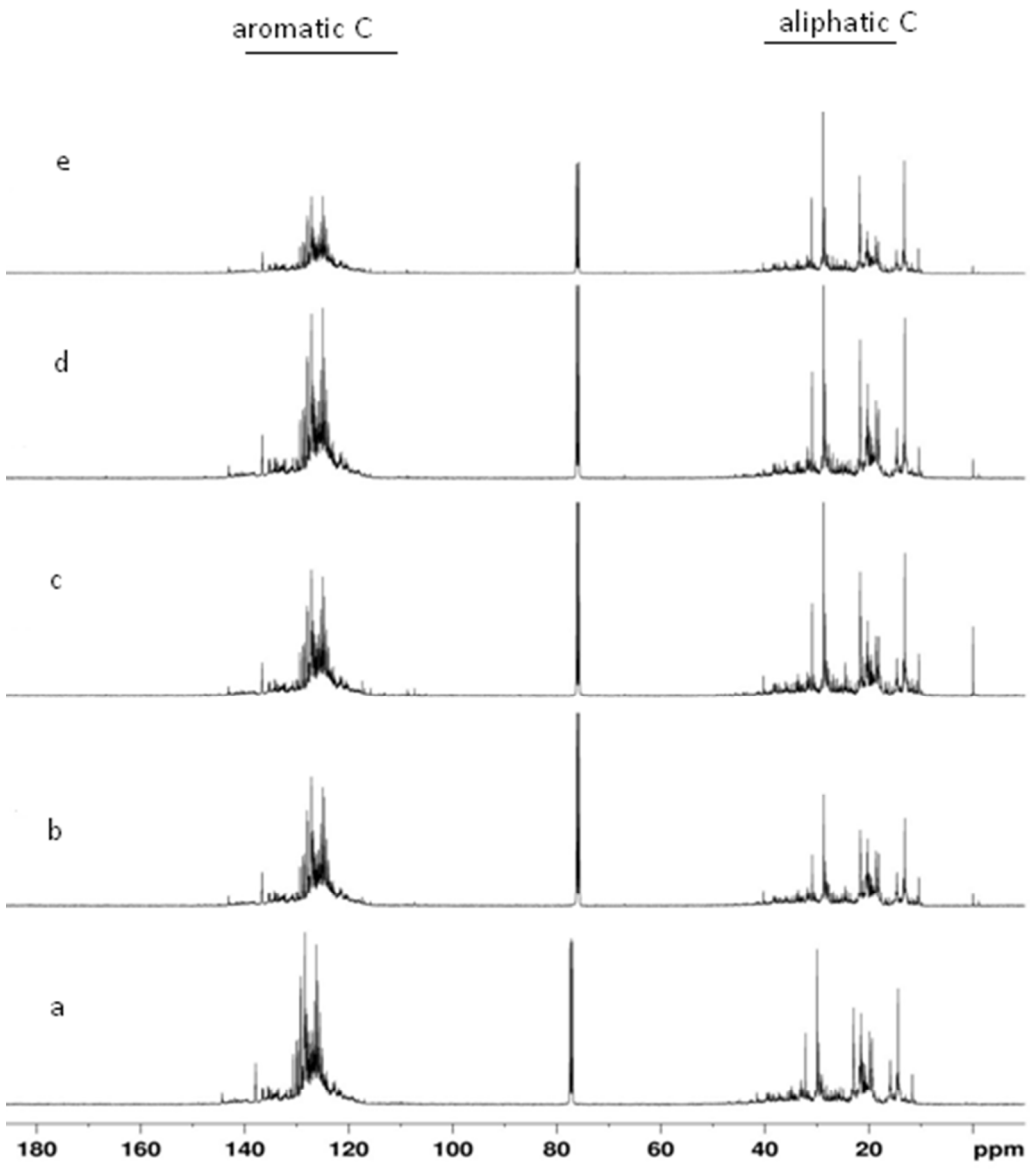

Figure 8: ^{13}C NMR of FCC liquid distillates on co-processing of FPO with VGO in a blending ratio of (a) 5:95; (b) 10:90; (c) 15:85; (d) 20:80 and (e) co-processing of HDO oil with VGO in a blending ratio of 5:95